

# Uncertainty Visualization using HDR Volume Rendering

Vijeth Dinesha · Neeharika Adabala · Vijay Natarajan

Received: date / Accepted: date

**Abstract** In this paper, we explore a novel idea of using high dynamic range (HDR) technology for uncertainty visualization. We focus on scalar volumetric data sets where every data point is associated with scalar uncertainty. We design a transfer function that maps each data point to a color in HDR space. The luminance component of the color is exploited to capture uncertainty. We modify existing tone mapping techniques and suitably integrate them with volume ray casting to obtain a low dynamic range (LDR) image. The resulting image is displayed on a conventional 8-bits-per-channel display device. The usage of HDR mapping reveals fine details in uncertainty distribution and enables the users to interactively study the data in the context of corresponding uncertainty information. We demonstrate the utility of our method and evaluate the results using data sets from ocean modeling.

**Keywords** Uncertainty visualization · Transfer function design · Ray casting · Volume rendering · High dynamic range imaging · Tone mapping

---

V. Dinesha  
Department of Computer Science and Automation,  
Indian Institute of Science, Bangalore, India  
E-mail: vijeth.d@csa.iisc.ernet.in

N. Adabala  
CybULab, 525, Anandanilayam, 5th Cross,  
JRD Tatanagar, Bangalore, India  
E-mail: neeharik@gmail.com

V. Natarajan  
Department of Computer Science and Automation,  
Supercomputer Education and Research Centre,  
Indian Institute of Science, Bangalore, India  
E-mail: vijayn@csa.iisc.ernet.in

## 1 Introduction

Data sets in science and engineering often have ancillary uncertainty information. The uncertainty may refer to various quantities associated with data including error, accuracy, variability, noise, or completeness of the data. These uncertainties usually arise due to errors in data acquisition and data processing. When visual analysis is used to interpret the data, it is important to communicate the associated uncertainty information, as it enables users to be conscious of the confidence of interpretations of the data and decisions made based on the visualization.

Various approaches may be used to quantify and represent uncertainty depending on its nature [1]. For example, it can be represented by a scalar or a multi-dimensional vector. In this paper, we focus on the use of a scalar value to represent uncertainty. The scalar value could be the confidence level, variability, or error associated with the scalar data.

Simple methods such as error bars and box plots are effective for visualizing scalar uncertainty in 1D scalar fields. Various uncertainty visualization methods have been studied for scalar data over 2D surfaces [2–5]. In this work we are interested in 3D data where each point in the domain volume has an associated scalar data value and a corresponding value for the uncertainty. The above mentioned 1D and 2D methods are not directly applicable to the 3D cases. Existing methods for uncertainty visualization in 3D often modify a basic visualization method by introducing glyphs or textures to convey uncertainty [6]. These methods can represent only coarse details in uncertainty, and lead to visual clutter when detailed visualizations are attempted.

In this paper, we propose an uncertainty visualization method based on direct volume rendering. Volume

rendering [7] is a classical method used to visualize 3D scalar fields, where the volume is projected onto the screen. An important step in the volume rendering process is the definition of a transfer function that maps the data points to visual attributes like color and opacity. Typically, a color is represented using three primary components namely red, green, and blue. When data is combined with the associated uncertainty, it increases the amount of information to be conveyed visually. A standard scheme for encoding colors, with 8-bit channels for each of the RGB components, forces considerable approximations in both uncertainty and data values. This causes the resulting visualization to suffer from loss in details. We overcome this limitation by employing High Dynamic Range (HDR) technology.

The ratio of maximum luminance to the minimum non-zero luminance of colors in an image or a scene is referred to as its dynamic range. There is a limit to the maximum dynamic range of any digital image inherently imposed by the color representation that it uses. The conventional color representation with one byte to encode each color component does not capture the entire dynamic range of a typical natural scene, which is about  $10^5 : 1$ . HDR imaging uses floating point color components and hence can be used to capture all the perceivable information in most natural scenes. However, a HDR image cannot be directly displayed on a typical display device such as a CRT monitor whose dynamic range is limited. To overcome this limitation, tone mapping techniques are employed to generate Low Dynamic Range (LDR) images that preserve most of the details present in the HDR image.

We propose the use of colors in HDR space to design transfer functions that capture detailed variation in both data and uncertainty. To achieve this, we represent the uncertainty in the luminance component of color. Luminance of a color is an approximate measure of how bright it appears. We apply tone mapping techniques in our visualization pipeline to preserve the details in uncertainty while creating a LDR representation of the data. This LDR image can be displayed on conventional 8-bits-per-channel display devices.

A good visualization method for uncertainty should not only create detailed visuals but also allow the users to explore the data and enable answering queries like: *What are the regions of high or low uncertainty in the domain?* and *What is the distribution of uncertainty within a given spatial region of interest?* We design a software tool for uncertainty visualization that supports user interactions and provides the necessary framework to answer queries of the kind mentioned above.

The main contributions of this paper are:

- Design of a suitable transfer function that maps data and uncertainty into HDR colors, making it possible to capture details in both data and uncertainty in the visualization.
- Modification of the HDR volume visualization pipeline [8,9] specifically to address the problem of uncertainty visualization. Our modifications allow for faster user interaction with the visualization.
- Definition of an interaction scheme with the rendered visualization to enable data and uncertainty exploration. This serves as a powerful tool to make inferences under circumstances where the knowledge of uncertainty contributes to deeper insights into the data.

The outline of the rest of this paper is as follows. In Section 2, we present previous work related to uncertainty visualization and also provide an overview of prior work in HDR imaging. In Section 3, we explain our uncertainty visualization method in detail and provide implementation details. In Section 4, we discuss applications of our approach and demonstrate results on data sets from ocean modeling. In Section 5, we summarize our technique and conclude with directions for future work.

## 2 Related Work

Literature pertinent to the techniques presented in this paper fall into two main categories: uncertainty visualization techniques, and HDR Imaging and HDR volume visualization techniques. We briefly outline prior work done in each of these areas below.

### 2.1 Uncertainty Visualization

Uncertainty visualization research has gained momentum in the visualization community since the work of Johnson and Sanderson [10] that emphasized its significance.

Pang et al. [11] present how significant amounts of uncertainty are often introduced in the process of simulation and data acquisition due to usage of different approximation algorithms and interpolation methods in data processing and visualization. Their work also presents a variety of techniques suitable for visualizing the introduced uncertainty. These techniques include addition and modification of geometry and attributes, animation, sonification, and psychovisual methods. However, these methods are not applicable to 3D scalar data sets with uncertainty.

Lodha et al. [12] used glyphs to visualize uncertainty in scalar fields. Wittenbrink et al. [13] studied vector

fields on surfaces and used glyphs for visualization of uncertainty in magnitude as well as direction of vectors. A drawback of these methods is that the glyphs can only be placed at discrete grid points and hence can not display detailed variations in uncertainty without visual clutter.

There has been a considerable amount of research done on uncertainty visualization of scalar fields over 2D surfaces. The work of Cedilnik and Rheingans [2] describes a technique with minimal interference. They employed procedural techniques to distort geometric primitives like grids that annotate the data. Grigoryan and Rheingans [3] addressed the problem of visualizing surface uncertainty by rendering the surface as a collection of points and displacing each point from its original location along the surface normal by an amount proportional to the uncertainty at that point. Lee and Varshney [4] described the visualization of molecular surfaces whose position is uncertain due to thermal vibrations. They generated fuzzy surfaces by rendering multiple layers of transparent surfaces at different configurations formed by vibrating points. The transparency of a point in a layer is decided by the confidence level of its position.

Haroz et al. [14] describe an interactive technique for visualizing bounded (location) uncertainty and unbounded (velocity) uncertainty associated with time-variant cosmological particles that occupy a volume. The technique renders a distribution of particles rather than a volume, and encodes uncertainty in the color of the particles. This primary spatial visualization of the particle locations is augmented with a parallel coordinates view of the data that enables user interaction and selection of regions of interest.

Though these methods are effective for visualization of surface uncertainty or discrete particle sets, they are not directly applicable to volume rendering of 3D scalar fields. Djurcilov et al. [6] identified this drawback and presented a direct volume rendering approach for visualizing scalar volumetric data with uncertainty information. They discussed postprocessing of the rendered volume by introducing discontinuities such as speckles, depth shaded holes, adding noise, and using textures to represent the uncertainty. Studying detailed variations in uncertainty using this method requires the introduction of noise textures during post-processing, which often results in visual clutter. Lundström et al. [15] explore detailed variations in uncertainty using animation but uncontrolled movement and flickering of the image causes visual fatigue.

These limitations can be overcome by using color to encode uncertainty in data. This is explored by Hengl [5], who used the HSI color space to visualize uncertain 2D

geographic data sets. The hue was chosen based on the scalar value and luminance was defined as a function of uncertainty. However, the number of colors available in HSI space are too few to capture the detailed variation in the scalar values and uncertainty while dealing with three dimensional data. We overcome this limitation by using HDR image techniques. In recent work, we explored the feasibility of applying HDR image maps for uncertainty visualization and presented some preliminary results [16]. In this paper, we develop a complete uncertainty visualization method by designing a HDR transfer function that maps the scalar data values and uncertainty into the high dynamic range colors. We then develop a renderer that is able to take this representation and create visualizations that preserve the detailed variation in data and uncertainty. We apply optimizations to the visualization pipeline to make interaction with the visualization feasible and create a tool that enables data exploration and examination based on specific queries. The interaction enhances the understanding of the data.

Sanyal et al. [17] presented a user study to compare four uncertainty visualization techniques that are applied to 1D and 2D synthetic datasets. In conclusion, they acknowledge that data from real sources has its merits because it can establish direct returns from results of a user-study. We evaluate our proposed technique using data studied by oceanographers and verify whether an expert in the field is able to make meaningful inferences based on the visualizations that we generate.

## 2.2 HDR imaging and HDR volume visualization

Debevec and Malik [18] introduced the concept of HDR imaging by developing a mechanism to recover and represent HDR radiance maps from a sequence of LDR photographs of a scene captured at different exposures.

Typical display devices are not capable of displaying images with dynamic range more than 1000 : 1. Therefore tone mapping algorithms have been developed to enable the viewing of HDR images on LDR (Low dynamic Range) display devices. The tone mapping algorithms are inspired by concepts in image processing, photography and human visual system modeling. Apart from reducing dynamic range, the tone mapping operators attempt to provoke same perceptual responses as when viewing a HDR scene in the real world. Tone mapping algorithms can be broadly classified into two categories:

- *Global tone operators*: where the same transformation is applied to color at every pixel in the im-

age [19–21]. The transformation is typically non-linear and depends on the properties of the image as a whole.

- *Local tone operators*: where the dynamic range of the image is reduced by a transformation which is not spatially uniform. These operators exploit the fact that perception of color at a pixel is mainly influenced by the surrounding colors. Variants of image processing techniques such as adaptive histogram equalization [22] and bilateral filtering are employed to perform the tone mapping. The contrast reduction applied at a pixel is usually determined by its local neighborhood [23–26].

The use of HDR technology in visualization is relatively recent and the benefits of using HDRI are yet to be studied extensively. Ghosh et al. [27] used HDR display technology for volume rendering. Yuan et al. [8, 9] used volume rendering with colors in extended dynamic range especially for visualization of high precision scalar volumetric data sets with high spatial resolution. They used floating point color components in transfer function design to allow for HDR luminance values. Tone mapping methods were used to display the volume rendered HDR image on conventional display devices. In this paper, we focus on using HDR volume rendering to create and interact with visualizations of scalar field with uncertainty. We present details of our approach in the following section.

### 3 Our approach

We work with 3D scalar data sets in form of rectilinear grids where a pair of scalars  $(\mu_p, \sigma_p)$  is available at every grid point  $p$ , representing the data value and uncertainty respectively. The scalar and uncertainty values at intermediate locations of the grid points are obtained by trilinear interpolation within the voxel. A schematic diagram of our visualization method is shown in Figure 1. It has two important modules:

1. *HDR Transfer Function designer*

This involves mapping a data point to color and opacity. A good transfer function captures all important details in data and uncertainty.

2. *HDR Volume Renderer*

The application of transfer function on the data set yields a 3D color volume possibly with a high dynamic range. We use ray casting and tone mapping methods to produce a volume rendered image that can be displayed on a conventional display device with limited dynamic range.

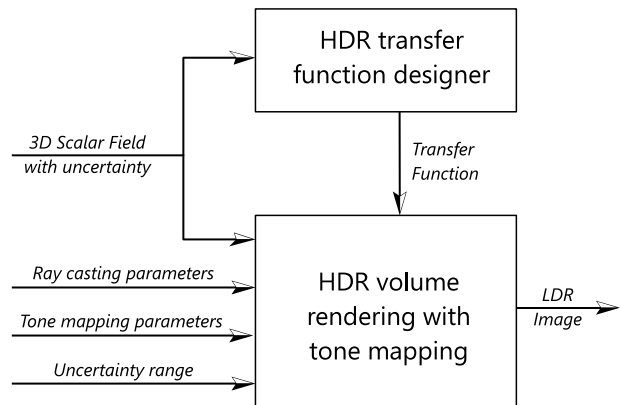


**Fig. 1** Schematic diagram of our visualization method using HDR volume rendering.

We now discuss each of these modules in detail.

#### 3.1 HDR transfer function designer

The quality of a volume rendered image is mainly determined by the transfer function used. Hence, transfer function design plays an important role in any visualization method that involves direct volume rendering.

We use CIELAB color space to encode a color. In this space, a color is represented by a lightness component  $(L^*)$ , a pair of chromaticity components  $(a^*, b^*)$  and an opacity component  $(\alpha)$ , each of which is a single precision floating point number. The CIELAB color space is selected because it closely approximates a perceptually uniform color space, where uniform changes in values of  $L^*$ ,  $a^*$ , or  $b^*$  result in uniform changes in color perceived [28]. Though it is not used routinely for volume rendering, the CIELAB color space has unique properties that have been leveraged in the context of generating harmonic colormaps for volume visualization [29]. In this color space, hue of a color depends on its chromaticity components and the luminance depends on its lightness component. Perceptual research indicates that hue plays a major role in visual grouping. However, if we use different hues to represent data and uncertainty, it results in insufficient number of colors to encode all the information. Therefore, we use hue property to represent only the scalar value. We use luminance component to encode uncertainty. The use of floating point color components gives us a wide range of luminance values to encode uncertainty, and thus allows the user to study fine details in uncertainty distribution. Figure 2 illustrates this approach to define the mapping between data values and color.

We allow the user to specify a map from scalar value  $\mu_p$  at point  $p$  to chromaticity  $(a_p, b_p)$  and opacity  $\alpha_p$

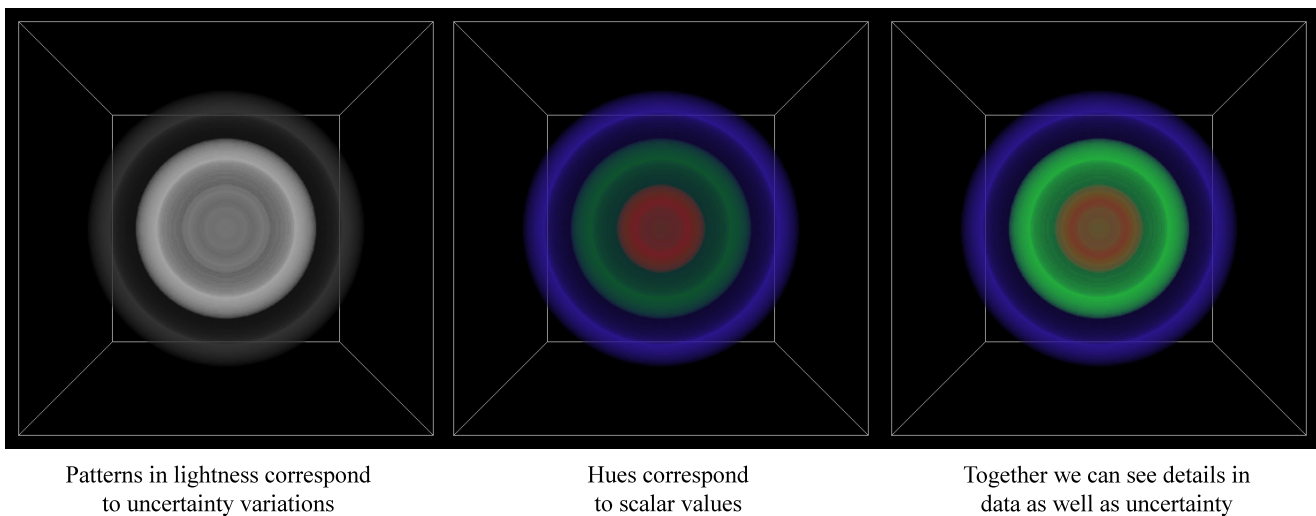


**Fig. 2** Visualization of a synthetic data set consisting of three concentric spheres having different scalar values. Different hues distinguish these scalar values. Lightness is defined to be proportional to uncertainty. We can see that the uncertainty of the green sphere is higher compared to the other two.

components. A suitable method can be used to define this mapping depending on the kind of data being visualized. For example, if one is interested in identifying the structure of different materials in the volume, a multidimensional transfer function to enhance material boundaries [30] can be used.

We determine lightness component  $L_p^*$  of the color based on uncertainty  $\sigma_p$  at point  $p$ . For generic data sets, we observe that it is useful to define lightness at a point  $p$  as

$$L_p^* = C \cdot L_R^* \cdot \left( \frac{\sigma_p - \sigma_{min}}{\sigma_{max} - \sigma_{min}} \right), \quad (1)$$

where  $L_R^*$  is defined to be 100, the lightness of the reference white. We use CIE standard illuminant D50 (with CIEXYZ components being 0.96422, 1.00000, and 0.82521) as reference white in the equations for color space transformation.

$\sigma_{max}$  and  $\sigma_{min}$  are the maximum and minimum values of uncertainty in the volume, and  $C$  is the proportionality constant interactively set by the user. As the value of  $C$  increases, uncertain regions are mapped to brighter colors.

To assist users in exploring the data better, we allow a uncertainty range of interest to be specified. The points that do not have uncertainty in this range are made invisible by making them transparent ( $\alpha_p = 0$ ). Depending on the application domain and kind of queries posed on the uncertainty distribution, alternative mappings for lightness may be used.

### 3.2 HDR volume renderer

We use ray casting [7] to render the volume on the view plane. Since we use colors in HDR space, it is necessary to incorporate tone mapping in the visualization process to generate images that can be displayed on conventional display devices.

A straightforward way to achieve this is to use the HDR volume visualization pipeline [8,9] introduced by Yuan et al. It involves casting a ray through the volume for every pixel in the view plane, and blending colors along the ray to obtain the color at the pixel. The dynamic range of the resulting image is determined by the distribution of uncertainty in the volume, and hence can be very high. An existing tone mapping algorithm can be applied to reduce this dynamic range and display the resulting image on screen. This model is shown in Figure 3.

It is possible to define an alternative approach to rendering, which is more effective in our case, by exploiting the way in which the transfer function is designed. Since  $L_p^*$  at an arbitrary point  $p$  in the domain is defined as a linear function of  $\sigma_p$ , it can be obtained by trilinear interpolation of lightness values associated with corners of the voxel containing  $p$ . This is not true in general for simple volume rendering of a scalar field with a user-specified transfer function. In our case, we can pre-shade the lightness values without losing details. In other words, we can initially obtain a HDR lightness field by mapping every grid point into a lightness value. We can then apply tone mapping on this 3D field instead of applying it on the final image. The result is a regular 3D grid of lightness values which

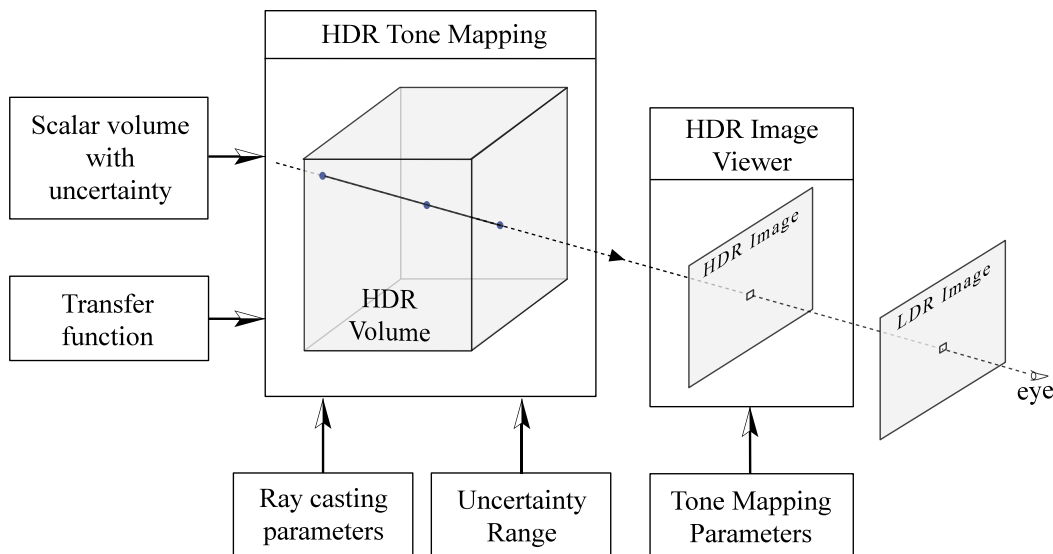


Fig. 3 Schematic of the HDR volume visualization pipeline.

constitutes a LDR lightness field with most details preserved. While ray casting, we obtain the  $L_p^*$  value at a point  $p$  by interpolating the tone mapped lightness values. This model is shown in Figure 4, and helps us improve upon the earlier model in following respects.

1. Typically, a tone operator applies a parametric function on color at every pixel in the 2D image to reduce its dynamic range. Most of the existing algorithms configure themselves and choose optimal parameters adaptively depending on the input image to preserve most details in the resulting LDR image. Though we have a 2D image as a result of ray casting, it is essentially a visualization of the volumetric data. Different images are produced when user interacts with the visualization by rotating or scaling the volume. It is important to use same tone mapping parameters for all these images to avoid any inconsistency in visualization.
2. Local tone operators typically rely on the properties of local neighborhood of a pixel and apply suitable transformation on the pixel. When the points are in 3D domain, it is better to study their neighborhood properties in 3D.
3. In our model, tone mapping is applied only once during initialization. While the user is interacting with the visualization, any existing methods like ray casting or splatting can be directly used to render the volume. This allows for efficient user interaction with the visualization without any additional overhead of tone mapping. In fact, we can think of the pre-shading of lightness values followed by tone mapping, and the user-specified transfer function for

hues as collectively constituting a simple transfer function.

Our tone mapping method for 3D is based on the algorithm described by Durand and Dorsey for images [24]. Initially, we obtain  $L^*$  values at grid points using equation 1 with constant  $C$  set to one. We use  $C$  to scale the lightness values after tone mapping. Therefore lightness at a grid point  $p$  is given by:

$$L_p^* = L_R^* \left( \frac{\sigma_p - \sigma_{min}}{\sigma_{max} - \sigma_{min}} \right) \quad (2)$$

We perform tone mapping on the logarithm of  $L^*$  values as differences in logarithmic scale correspond to contrast ratios,  $L_p = \log L_p^*$ . An edge preserving bilateral filter is applied on  $L$  values to obtain a *base field*,  $B$ :

$$B_p = \frac{1}{k(p)} \sum_{y \in \Omega} f(\|y - p\|) g(L_y - L_p) L_y \quad (3)$$

where  $\Omega$  is the set of all grid points in the 3D domain and  $k(p)$  is the normalization factor,

$$k(p) = \sum_{y \in \Omega} f(\|y - p\|) g(L_y - L_p) \quad (4)$$

Bilateral filter effectively blurs the input while preserving sharp edges (or surfaces). We use Gaussian functions for  $f$  and  $g$  in spatial domain and lightness domain respectively. We restrict  $\Omega$  to be the set of grid points in the local neighborhood of  $p$  as the remaining points do not contribute significantly to the summation.

The difference between  $L_p$  and  $B_p$  is referred to as detail at point  $p$ . The detail field contains most of the fine details in the distribution and its dynamic range

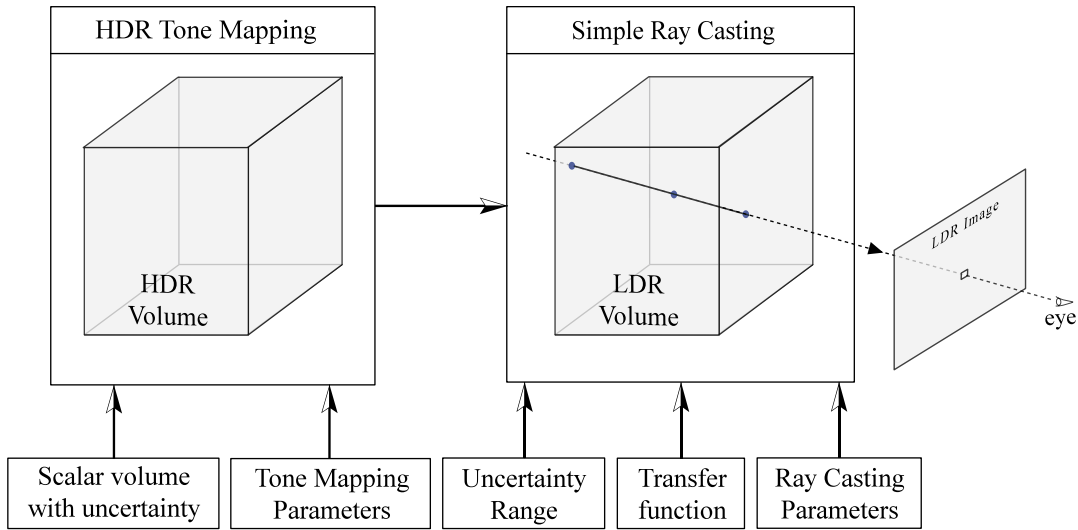


Fig. 4 Schematic of our improved HDR ray casting-based pipeline for uncertainty visualization.

is typically low. Dynamic range reduction is applied on base field using an appropriate scaling factor  $s$ . The tone mapped lightness values  $L'_p$  are obtained by exponentiating the sum of detail values and the scaled base values.

$$L'_p = e^{(L_p - B_p(1-s))} \quad (5)$$

The resulting LDR lightness field is stored in memory and is used whenever the volume needs to be rendered.

We use ray casting to render the volume on screen.

1. Points are sampled at regular intervals in the volume along rays that pass through every pixel  $x$  on the image.
2. Lightness at a sampled point  $q$  is obtained by trilinear interpolation of tone mapped lightness values. The lightness value is scaled by a user specified constant  $C$  and a small bias (20% of the lightness of reference white) is added to avoid dark colors:

$$\tilde{L}_q^* = 0.2 L_R^* + 0.8 C L'_q \quad (6)$$

3. The chromaticity ( $a_q^*, b_q^*$ ) and opacity  $\alpha_q$  at  $q$  is obtained from the transfer function based on scalar value at  $q$ .
4. The color ( $\tilde{L}_q^*, a_q^*, b_q^*$ ) is transformed to RGB color space to obtain  $(R_q, G_q, B_q)$ . The components  $R_q, G_q$  and  $B_q$  are scaled by  $\alpha_q$ . The RGB colors along a ray, thus obtained are accumulated using the volume rendering integral to obtain the final pixel color  $(R_x, G_x, B_x)$ .

$$\begin{aligned} R_x &\leftarrow R_x + (1 - \alpha_{ray}) \alpha_q R_q \\ G_x &\leftarrow G_x + (1 - \alpha_{ray}) \alpha_q G_q \\ B_x &\leftarrow B_x + (1 - \alpha_{ray}) \alpha_q B_q \\ \alpha_{ray} &\leftarrow \alpha_{ray} + (1 - \alpha_{ray}) \alpha_q \end{aligned} \quad (7)$$

When  $C$  is less than one, the RGB components at every pixel lie within the range zero to one. As the value of  $C$  is increased, the uncertain regions tend to saturate and become more visible.



Fig. 5 As the value of lightness is increased (from left to right), red hue tends to shift towards orange.

Our method has a minor drawback. Each hue has a threshold lightness beyond which it is not well-defined. In other words, as the lightness  $L^*$  of a color is increased keeping its chromaticity ( $a^*, b^*$ ) constant, beyond a certain point the colors do not have valid equivalents in RGB space. For example, in Figure 5 we see that the red hue is defined for values of lightness only up to about 54% of reference white. In such cases, when we clamp the RGB values to be within zero to one, a slight hue shift is introduced. This effect is apparent in Figure 16 where we observe hue shift from red to orange and blue to purple in regions of high uncertainty.

### 3.3 Implementation details

We have developed a visualization tool to demonstrate the usability of our method. The scalar field and corresponding uncertainty field are loaded in the form of 3D grids from separate files having the same dimensions. Histogram of the scalar values is presented to the user. We obtain mappings for chromaticity and opacity from the user as a function of scalar values. Figures 6 and 7

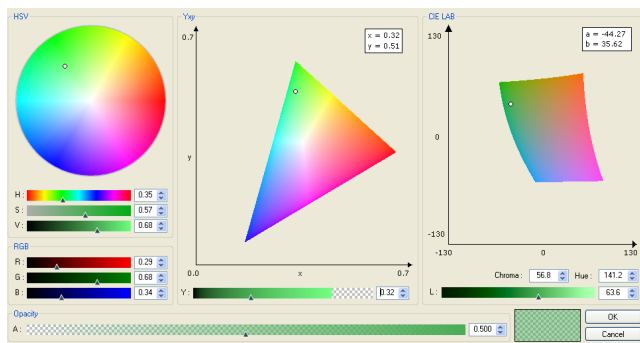


Fig. 6 User interface for color selection

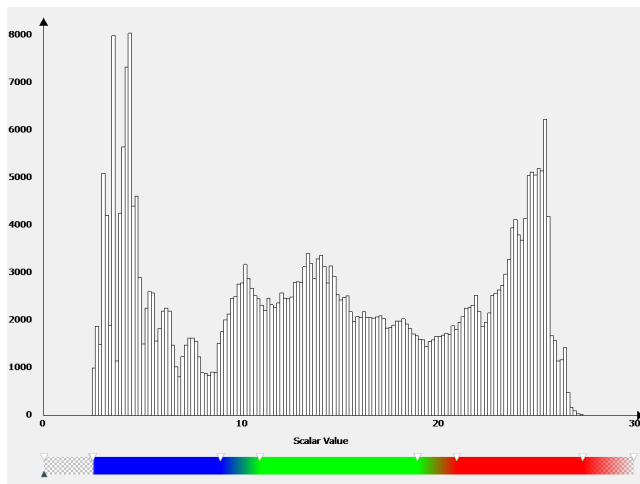


Fig. 7 Transfer Function Designer

show the user interface provided for color selection and hue transfer function design respectively.

The uncertainty values at grid points are mapped to lightness values and tone mapping is performed. The resulting lightness field serves as input to the ray casting module. Ray casting is implemented in hardware using OpenGL fragment shaders to render the volume at interactive speeds. A user perceives depth information by rotating and zooming in/out of the volume using a virtual trackball interface. The visual effect of uncertainty is controlled by interactively modifying the constant  $C$ . Users can explore the data set in uncertainty space by specifying uncertainty range of interest. Further, we enable users to study data or uncertainty patterns independently by rendering with a constant function for lightness, or by disabling hues respectively.

## 4 Results and discussion

We use geo-spatial data sets from ocean modeling to evaluate our visualization method. In the following subsections, we study ocean temperature and salinity fields measured in the Middle Atlantic Bight (MAB) region

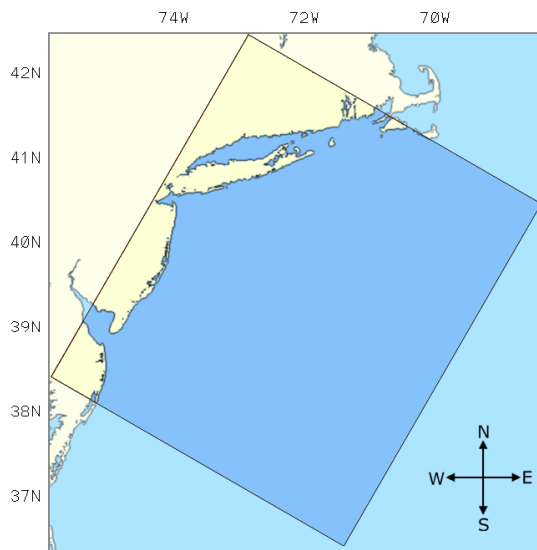


Fig. 8 MAB region with land and sea shown in different colors. Highlighted rectangle shows the region where temperature and salinity measurements are available.

and in the Bay of Bengal region. The interpretations are based on discussions with an oceanographer at Indian Institute of Science, Bangalore.

The preprocessing of lightness values to generate the LDR volume is implemented by applying bilateral filtering to 125 grid points in the neighborhood of each point. Our current implementation is in the CPU and it is found to take about 2.2 seconds for preprocessing the Bay of Bengal data set and about 8 seconds for the Mid-Atlantic Bight data set. No optimizations were applied to the implementation, there is scope to achieve better performance by implementing the algorithm in hardware. After the preprocessing, we achieve a frame rate of 20 fps for a resolution of  $650 \times 650$  on a NVIDIA 8800 GTX graphics card with a ray casting sampling step size of 0.1% of volume dimensions. A simple volume of scalar values can be rendered without uncertainty based lightness processing at a rate of 50 fps. We observed frame rates of about 40 fps with a step size of 1% of volume dimensions.

### 4.1 Results on Middle Atlantic Bight data

The data [31] consists of physical variables including temperature and salinity measured on the Middle Atlantic Bight (MAB) south of New England, off the east coast of the United States. Measurements are taken at hourly intervals and at different depth levels. Figure 8 shows the extent of the data set in the MAB region. We visualize first 15 depth levels which consists of data up to 200m deep from the surface. Data within each level is sampled on a regular  $149 \times 175$  sized grid with each

measurement being a floating point value accurate up to three decimal places. We compute the mean and standard deviation of the hourly measurements over a day and consider the resulting values as scalar field and its uncertainty respectively. The range of scalar values and uncertainty in the resulting dataset is given in Table 1. In this application, uncertainty refers to variability of the scalar values over a day.

	Minimum	Maximum
Temperature field	5.891°C	27.417°C
Temperature Uncertainty	0.004°C	3.532°C
Salinity field	29.255 g/L	36.461 g/L
Salinity Uncertainty	0.001 g/L	0.692 g/L

**Table 1** Range of values in Mid-Atlantic Bight data set.

Figure 9 shows visualization results on the MAB salinity field. It demonstrates how we can study the scalar field and corresponding uncertainty by representing them as hues and lightness respectively. The constant  $C$  allows users to control the effect of uncertainty field on the visualization as demonstrated in Figure 11 and the accompanying video. The scalar field distribution can be studied by setting  $C$  to a suitable low value where most hue patterns are clear. With the increase in  $C$ , the uncertain regions appear brighter and allow us to perceive uncertainty information. We also allow the users to study specific regions in the volume having uncertainty values within a range of interest as demonstrated in Figure 10. Since the scalar field and uncertainty each has a dynamic range of the order of  $10^3$ , HDR volume rendering enhances the quality of visualization considerably. This is demonstrated in Figures 13 and 14. The left image shows the rendering of temperature and salinity fields respectively with a lightness at each point determined by Equation 1 with  $C \approx 1.5$ . No preprocessing is applied on the lightness during ray casting and color composition is performed with 8-bit color components. The resulting color components at pixels are clamped to be within the displayable range. Lack of details in dark regions and presence of some bright regions illustrate that the data is of high dynamic range and calls for HDR methods to process the visualization. The middle image is rendered using our visualization pipeline. We can observe that the use of HDR tone mapping on the lightness field enhances details in dark regions as well as bright regions. The image in the right is generated by applying image based bilateral tone mapping on the final HDR image instead of initial preprocessing of lightness values in 3D. We observe that this image is not very different from the one rendered using our pipeline.



**Fig. 15** Highlighted rectangle shows the extent of the temperature and salinity data sets in the Bay of Bengal region. (Image source: Wikipedia)

The following are some of the inferences that can be made from the visualizations, which were validated by the oceanographer:

- We observe the low salinity waters near the shore mixing with the ocean waters having high salinity from Figures 9 and 10.
- The salinity field exhibits high uncertainty at the MAB shelf/drop off where the mixing is prominent. This is evident from Figure 10.
- We also infer that the regions of low uncertainty of salinity are found deep in the ocean from Figure 11.
- From Figure 12, we infer that the temperature near the ocean surface is higher compared to deeper regions. We see that the lightness channel effectively captures distribution of uncertainty. We note that regions of high uncertainty lie close to the surface especially near the MAB shelf, and correctly reflect the fact that interaction of water with the atmosphere and also the presence of currents on the surface lead to greater uncertainty in the temperature values.
- By choosing suitable uncertainty ranges of interest, we observe that the deeper regions in the ocean exhibit negligible deviation in temperature.

#### 4.2 Results on Bay of Bengal data

The data consists of daily measurements of salinity and temperature at different depth levels in the Bay of Bengal region ( $10^{\circ}N$  to  $25^{\circ}N$  and  $80^{\circ}E$  to  $100^{\circ}E$ ). This region is shown in Figure 15. We visualize the top 25

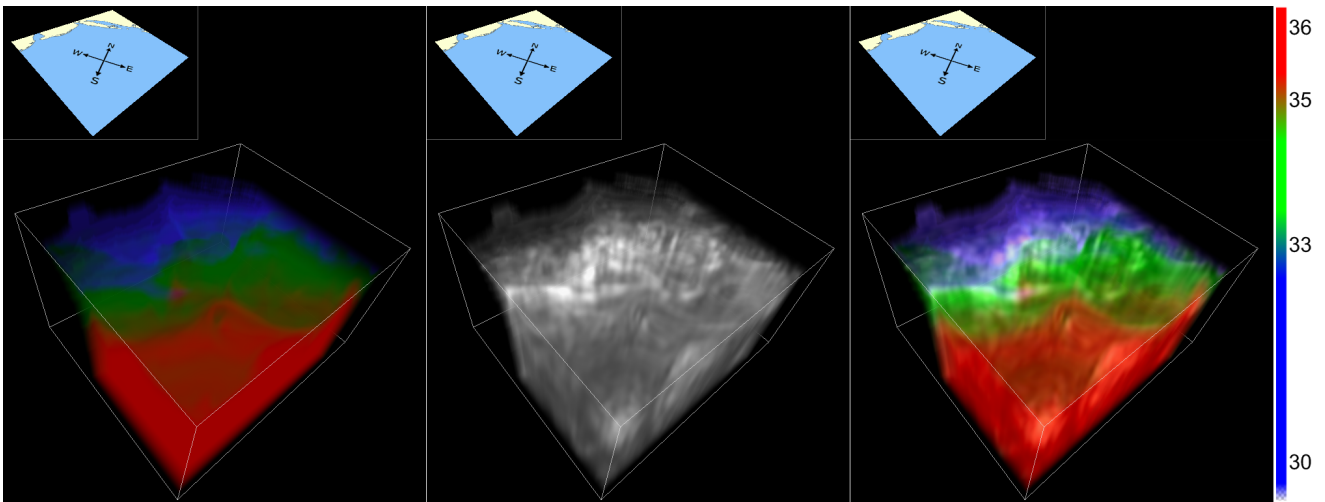


**Fig. 9** (Left) A simple volume rendering of the ocean salinity field, with all points mapped to a constant lightness of 0.35. (Middle) The patterns in lightness correspond to the uncertainty distribution. Higher the lightness, more uncertain the region is. (Right) Hue and lightness values together convey details in data as well as uncertainty.

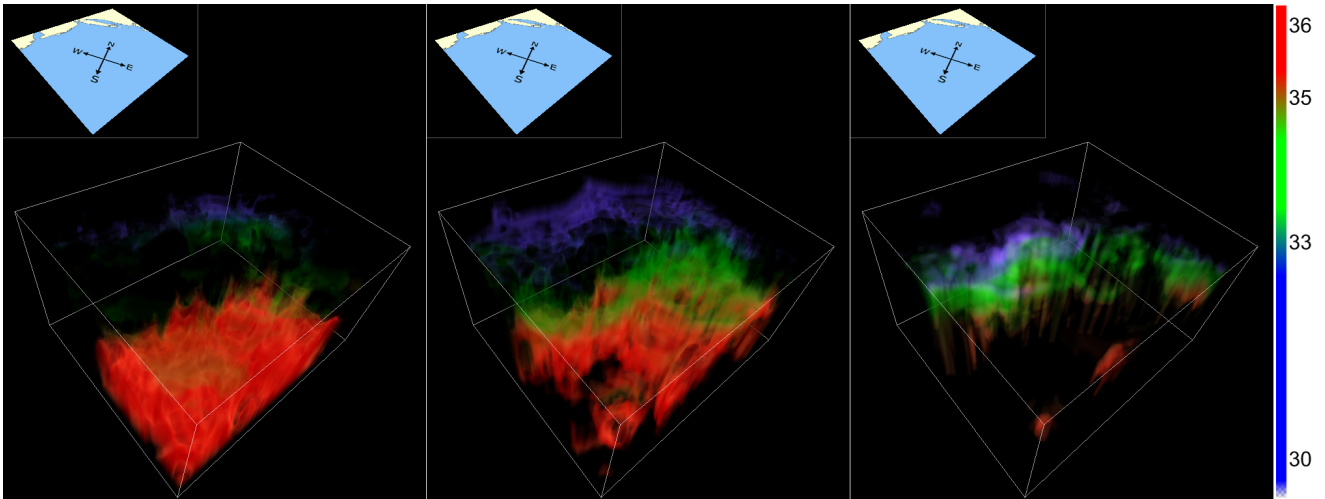


**Fig. 10** Regions of interest in the MAB salinity field having uncertainty values less than 0.025 gram per liter, in between 0.025 and 0.08 gram per liter, and greater than 0.08 gram per liter respectively from left to right.

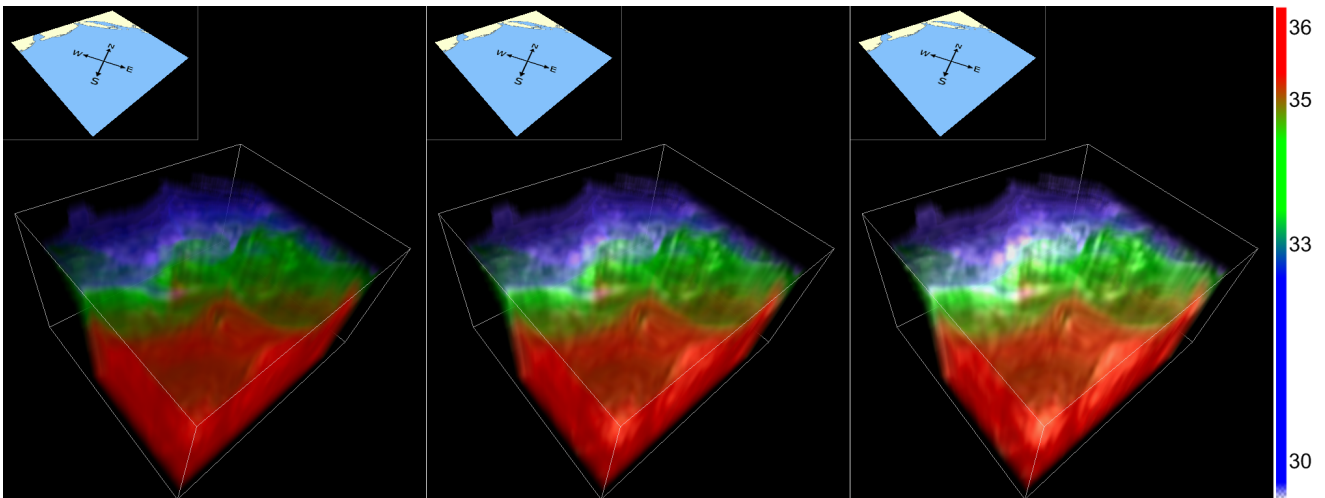


**Fig. 11** Effect of proportionality constant  $C$  on the visualization of the MAB salinity field. The uncertain regions saturate with increasing values of  $C$  (left to right). Deeper regions of the ocean remain dark indicating low uncertainty.

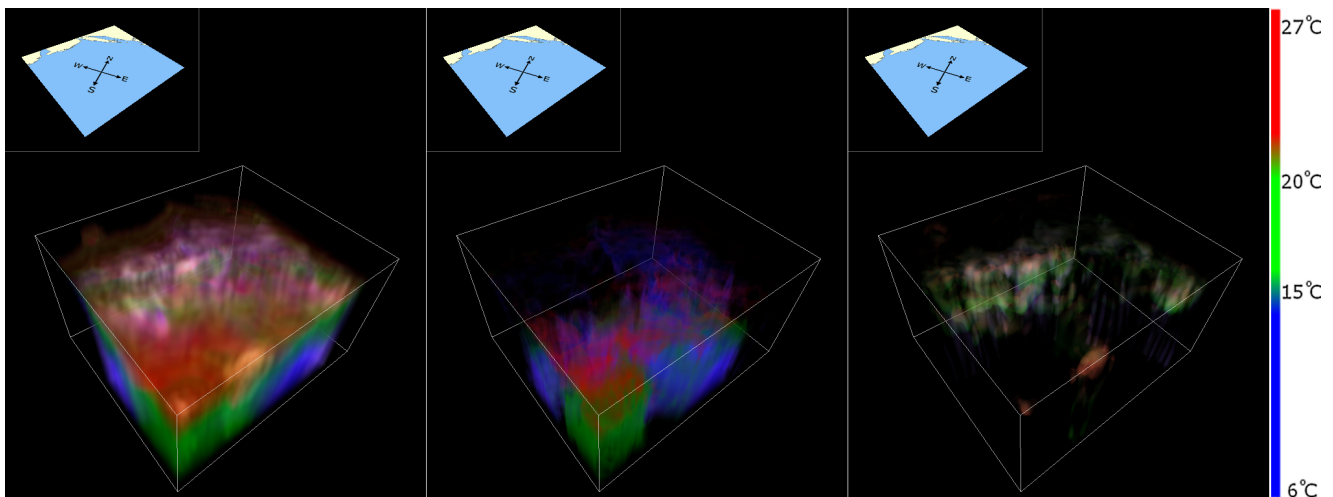


**Fig. 12** (Left) Uncertainty visualization of MAB temperature field. (Middle) Regions having uncertainty less than  $0.2^{\circ}C$ . (Right) Regions having uncertainty greater than  $0.5^{\circ}C$ . The temperature is high on the surface. Further, the uncertainty is also high near the ocean surface.

depth levels which constitute data up to 200m deep. Data within each level is sampled on a regular  $81 \times 61$  sized grid. We compute the mean and standard deviation of measurements over a year and consider the resulting values as scalar field and its uncertainty respectively. As in the previous case study, uncertainty here refers to variability of the temperature and salinity measurements over the year. The range of scalar values and uncertainty in the dataset is given in Table 2.

	Minimum	Maximum
Temperature field	14.145°C	29.135°C
Temperature Uncertainty	0.263°C	3.409°C
Salinity field	22.121 g/L	35.092 g/L
Salinity Uncertainty	0.002 g/L	3.949 g/L

**Table 2** Range of values in Bay of Bengal data set.

Figure 16 shows the distribution of salinity and its variation over a period of one year. We observe regions of low salinity in the North due to the inflow of fresh water from the river Ganga. We also observe that salinity increases with depth and in the south-west direction. In addition, from the same visualization, we are also able to observe that salinity varies more near the coast, again due to mixing with the river water and ocean currents that flow in the south west direction. Figure 17 shows the region with high variation in salinity. Figure 18 shows the temperature distribution and its variation during the year. We observe that the temperature decreases with depth is independent of latitude and longitude. The wedge shaped transparent region corresponds to Andaman and Nicobar islands. Temperature variation in the year is high towards the east and at a depth range of 50m-150m. This observation is validated

by the oceanographer’s knowledge of the region, and is due to the presence of waves with a large wavelength that cause a vertical shift of water. The temperature decreases rapidly in this depth range. So, the vertical shift causes the large variation during the year.

The oceanographer working with us on the study of both data sets found the visualizations helpful because they presented the scalar field distribution and the uncertainty in a unified view. The volume rendered images and the interactive tool provided a more intuitive visualization of the data compared to their existing scatter plot based visualization. It was clear that the ability to examine and explore the uncertainty in a scalar field was useful to make meaningful inferences from the data.

## 5 Conclusions and future work

We have developed a method to visualize scalar volumetric fields that allows users to explore the data in both uncertainty space and the scalar data space. The key contributions of our work are listed below:

1. A novel application of HDR technology for uncertainty visualization by encoding data as well as uncertainty using colors in HDR space. Our volume rendering-based method is able to display detailed variations in data as well as uncertainty. It overcomes the limitation of using uncertainty glyphs or noise textures that can lead to visual clutter. Our method is applicable to slices, isosurfaces, and scalar fields in lower dimensions.
2. Design of HDR transfer function that separates mappings for lightness and hue channels of color. The lightness is used to represent uncertainty, while hue

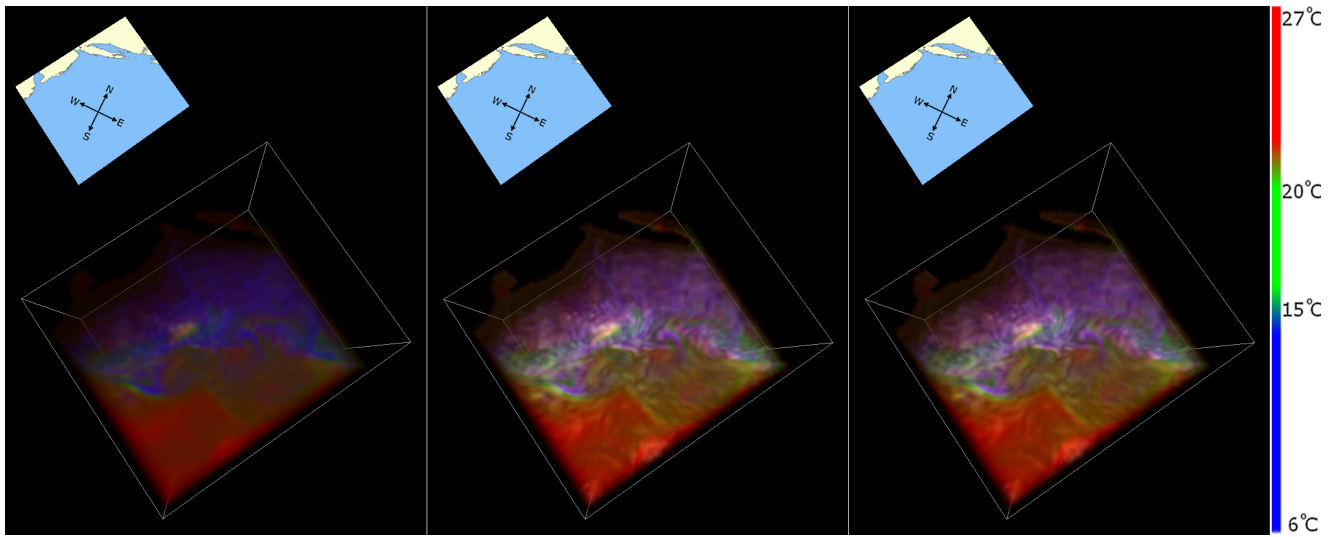


**Fig. 13** (Left) LDR rendering of the MAB temperature field. Lightness is determined using Equation 1. (Middle) HDR rendering of MAB temperature field with lightness preprocessing as per our visualization pipeline. (Right) HDR rendering of MAB temperature field. Tone mapping is applied on the final image instead of preprocessing lightness values in 3D.

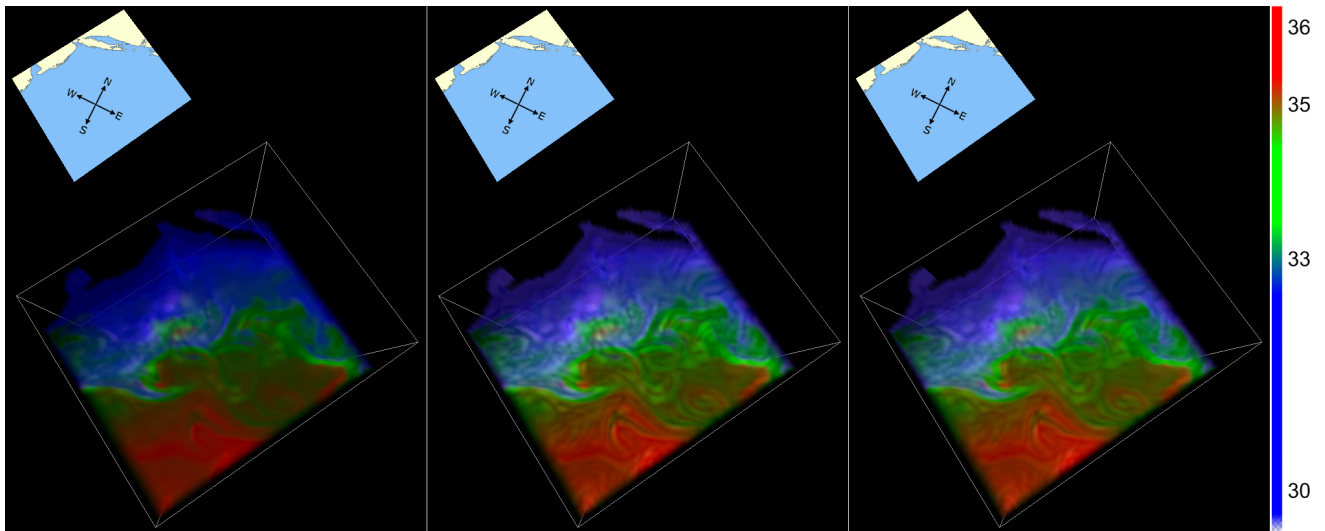


**Fig. 14** LDR rendering of the MAB salinity field. Lightness is determined using Equation 1. (Middle) HDR rendering of MAB salinity field with lightness preprocessing as per our visualization pipeline. (Right) HDR rendering of MAB salinity field. Tone mapping is applied on the final image instead of preprocessing the lightness values in 3D.

is used to represent the scalar value. This design enabled us to modify the existing HDR volume visualization pipeline by using pre-shading and tone mapping of lightness values in 3D, making the rendering process more efficient and making it possible to achieve real-time rendering speeds.

3. Development of an interface that supports user interaction with the uncertainty visualization and allows exploration of detailed variations in both data and uncertainty values. The process of interaction enabled highlighting the uncertainty by increasing the absolute values of lightness. The proposed technique enabled visualization of data based on uncer-

tainty ranges by manipulating transparency values of interactively selected regions.

We demonstrated the applicability of our approach using data sets from ocean modeling, and our interpretations of the visualizations were validated by an oceanographer.

As future work, we plan to explore alternate transfer function designs tailored to specific applications. It is possible to apply our method to analyze uncertainty in the context of specific measurement devices and define their characteristics. We believe that using HDR technology to enable perception of details in visualization can be extended to other attributes besides uncertainty.

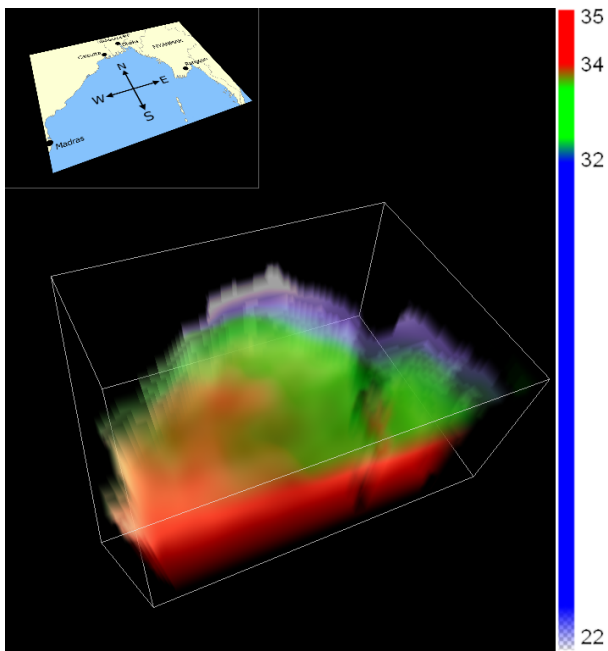


**Fig. 16** Uncertainty Visualization of Bay of Bengal salinity field. Salinity increases with depth and in the south-west direction. The uncertainty is high near the coast.

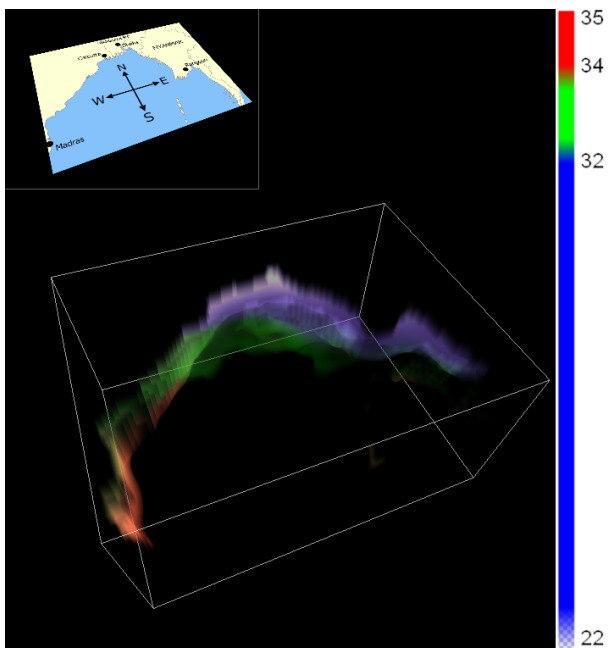


**Fig. 17** Regions in the Bay of Bengal salinity field having deviation greater than 0.5 gram per liter. The uncertainty is high along the coastal regions.

**Acknowledgements** We thank Prof. Vinayachandran for providing the Bay of Bengal data set and for his inputs on the study of the ocean data. We thank Prof. Lermusiaux for sharing the MAB data set. This work was supported by Microsoft Research India and by Department of Science and Technology, India under grant SR/S3/EECE/048/2007.

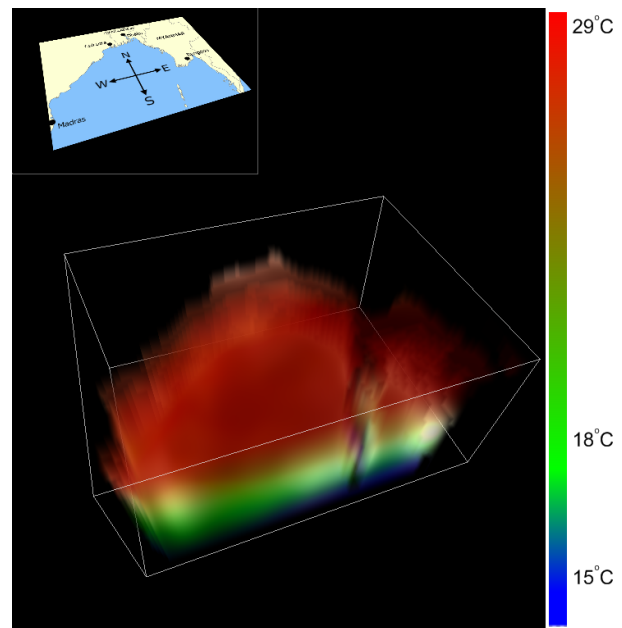


**Fig. 18** Uncertainty visualization of Bay of Bengal temperature field. Temperature decreases with depth. The uncertainty is high at depth ranges of 50m-150m and towards the east. The black wedge-like region towards the east is due to the Andaman and Nicobar Islands.

## References

1. Barry N. Taylor and Chris E. Kuyatt. Guidelines for evaluating and expressing the uncertainty of n.i.s.t. measurement results. Technical Note 1297, National Institute of Standards and Technology, Gaithersburg, MD, January 1993.
2. Andrej Cedilnik and Penny Rheingans. Procedural annotation of uncertain information. In *VIS '00: Proceedings of the IEEE Conference on Visualization '00*, pages 77–83, Los Alamitos, CA, USA, 2000. IEEE Computer Society Press.
3. Gevorg Grigoryan and Penny Rheingans. Point-based probabilistic surfaces to show surface uncertainty. *IEEE Transactions on Visualization and Computer Graphics*, 10(5):564–573, 2004.
4. Chang Ha Lee and Amitabh Varshney. Representing thermal vibrations and uncertainty in molecular surfaces. In *In SPIE Conference on Visualization and Data Analysis*, pages 80–90, 2002.
5. Tomislav Hengl. Visualisation of uncertainty using the hsi colour model: Computations with colours. *Proceedings of the 7th International Conference on GeoComputation*, pages CD–Rom, pp. 8–17, 2003.
6. Suzana Djurcilov, Kwansik Kim, Pierre Lermusiaux, and Alex Pang. Visualizing scalar volumetric data with uncertainty. *Computers & Graphics*, 26(2):239–248, 2002.
7. Paolo Sabella. A rendering algorithm for visualizing 3d scalar fields. In *SIGGRAPH '88: Proceedings of the 15th Annual Conference on Computer graphics and interactive techniques*, pages 51–58, New York, NY, USA, 1988. ACM.
8. Xiaoru Yuan, Minh X. Nguyen, Baoquan Chen, and David H. Porter. High dynamic range volume visualization. In *Proceedings of the IEEE Conference on Visualization 2005*, pages 327–334. IEEE Computer Society, 2005.
9. Xiaoru Yuan, Minh X. Nguyen, Baoquan Chen, and David H. Porter. Hdr volvis: High dynamic range volume visualization.

- IEEE Transactions on Visualization and Computer Graphics*, 12:433–445, 2006.
10. Chris R. Johnson and Allen R. Sanderson. A next step: Visualizing errors and uncertainty. *IEEE Comput. Graph. Appl.*, 23(5):6–10, 2003.
  11. Alex Pang, Craig Wittenbrink, and Suresh Lodha. Approaches to uncertainty visualization. *The Visual Computer*, 13(8):370–90, 1997.
  12. Suresh K. Lodha, Bob Sheehan, Alex T. Pang, and Craig M. Wittenbrink. Visualizing geometric uncertainty of surface interpolants. In *GI '96: Proceedings of the Conference on Graphics interface '96*, pages 238–245, Toronto, Ont., Canada, Canada, 1996. Canadian Information Processing Society.
  13. Craig M. Wittenbrink, Alex T. Pang, and Suresh K. Lodha. Glyphs for visualizing uncertainty in vector fields. *IEEE Transactions on Visualization and Computer Graphics*, 2(3):266–279, 1996.
  14. Steve Haroz, Kwan-Liu Ma, and Katrin Heitmann. Multiple uncertainties in time-variant cosmological particle data. In *Proceedings of IEEE Pacific Visualization Symposium*, pages 207–214, 2008.
  15. Claes Lundström, Patric Ljung, Anders Persson, and Anders Ynnerman. Uncertainty visualization in medical volume rendering using probabilistic animation. *IEEE Transactions on Visualization and Computer Graphics*, 13(6):1648–1655, 2007.
  16. Vijeth Dinesha, Neeharika Adabala, and Vijay Natarajan. Uncertainty visualization using hdr image maps. *Poster Abstracts at Eurographics/IEEE-VGTC Symposium on Visualization 2010, Eurographics*, June 2010.
  17. Jibonananda Sanyal, Song Zhang, Gargi Bhattacharya, Phil Amburn, and Robert Moorhead. A user study to compare four uncertainty visualization methods for 1d and 2d datasets. *IEEE Transactions on Visualization and Computer Graphics*, 15:1209–1218, 2009.
  18. Paul E. Debevec and Jitendra Malik. Recovering high dynamic range radiance maps from photographs. In *SIGGRAPH '97: Proceedings of the 24th Annual Conference on Computer graphics and interactive techniques*, pages 369–378, New York, NY, USA, 1997. ACM Press/Addison-Wesley Publishing Co.
  19. Frédo Durand and Julie Dorsey. Interactive tone mapping. In *Proceedings of the Eurographics Workshop on Rendering Techniques 2000*, pages 219–230, London, UK, 2000. Springer-Verlag.
  20. F. Drago, K. Myszkowski, T. Annen, and N. Chiba. Adaptive logarithmic mapping for displaying high contrast scenes. *Computer Graphics Forum*, 22:419–426, 2003.
  21. Kate Devlin. Dynamic range reduction inspired by photoreceptor physiology. *IEEE Transactions on Visualization and Computer Graphics*, 11(1):13–24, 2005.
  22. Stephen M. Pizer, E. Philip Amburn, John D. Austin, Robert Cromartie, Ari Geselowitz, Trey Greer, Bart Ter Haar Romeny, and John B. Zimmerman. Adaptive histogram equalization and its variations. *Comput. Vision Graph. Image Process.*, 39:355–368, September 1987.
  23. Erik Reinhard, Michael Stark, Peter Shirley, and James Ferwerda. Photographic tone reproduction for digital images. *ACM Trans. Graph.*, 21(3):267–276, 2002.
  24. Frédo Durand and Julie Dorsey. Fast bilateral filtering for the display of high-dynamic-range images. In *SIGGRAPH '02: Proceedings of the 29th Annual Conference on Computer graphics and interactive techniques*, pages 257–266, New York, NY, USA, 2002. ACM.
  25. Prasun Choudhury and Jack Tumblin. The trilateral filter for high contrast images and meshes. In *SIGGRAPH '05: ACM SIGGRAPH 2005 Courses*, page 5, New York, NY, USA, 2005. ACM.
  26. Raanan Fattal, Dani Lischinski, and Michael Werman. Gradient domain high dynamic range compression. In *SIGGRAPH '02: Proceedings of the 29th Annual Conference on Computer graphics and interactive techniques*, pages 249–256, New York, NY, USA, 2002. ACM.
  27. Abhijeet Ghosh, Matthew Trentacoste, and Wolfgang Heidrich. Volume rendering for high dynamic range displays. In *Volume Graphics*, pages 91–98, 2005.
  28. Mark D. Fairchild. *Color Appearance Models, Second Edition*. Wiley-IS&T Series in Imaging Science and Technology, Chichester, UK, 2005.
  29. L. Wang and K. Mueller. Harmonic colormaps for volume visualization. In *IEEE/EG Symposium on Volume Graphics*, pages 33–40, 2008.
  30. Joe Kniss, Gordon Kindlmann, and Charles Hansen. Interactive volume rendering using multi-dimensional transfer functions and direct manipulation widgets. In *VIS '01: Proceedings of the IEEE Conference on Visualization '01*, pages 255–262, Washington, DC, USA, 2001. IEEE Computer Society.
  31. Pierre F J Lermusiaux, Patrick J Haley Jr, Wayne G Leslie, and Oleg G. Logutov. Mseas re-analyses for the awacs-sw06 exercise in the middle atlantic bight region, 2008. <http://mseas.mit.edu/Research/AWACS/Model.Output/>.